

A Comparison of Three Boundary Layer Schemes for Numerical Weather Prediction

Marwa Farouk M. Ali^{1,*}, Zeinab Salah¹, Somaia A. Asklany², M. Hassan³, M. Harhash⁴ and M.M. Abdel Wahab⁴

¹Egyptian Meteorological Authority, Koubry El-Quobba, Cairo, Egypt

²Computer Science Department, Faculty of Science and Arts girl section, Northern Border University, Turaif, K.S.A

³Mathematics Department, Faculty of Science, Ain Shams University, Cairo, Egypt

⁴Astronomy, Space Science and Meteorology Department, Faculty of Science, Cairo University, Giza, Egypt

Received: 8 Jun. 2020, Revised: 2 Oct. 2020, Accepted: 10 Oct. 2020

Published online: 1 Nov. 2020

Abstract: Air pollution is a global issue that affects humans' health and economic growth. In the field of meteorology, numerical models play an essential role in weather and air quality forecast. For more accurate prediction of pollutants concentrations in the atmosphere, an efficient parameterization of the planetary boundary layer is required. In this paper, performances of three different planetary boundary layer schemes were investigated through estimating PM10 pollutant mass concentration during a sand storm using the regional climate model. Wind speed and planetary boundary layer height were also evaluated to examine the consistency of the model. The simulated results were validated by comparing the estimated values to the observed and reanalysis data. The results showed that the model provided good forecast for the dust event. However, one scheme had been recommended for predicting the PM10 concentration.

Keywords: Numerical weather models, Planetary Boundary schemes, Planetary Boundary layer height, PM10

1 Introduction

Mathematical models, algorithms and data structure play a very important role in several fields. In meteorology, some mathematical models were developed to forecast different weather phenomena that directly affect human life, health and activities [1]. Similar to weather forecast, mathematical simulations can predict the levels of airborne pollutants and air quality. One of these models is the regional climate model RegCM developed by the Earth Systems Physics group at the Abdus Salam International Centre for Theoretical Physics ICTP [2, 3, 4]. This model is based on fluid dynamics and some physical concepts. In such models, the dynamical equations of a compressible fluid are solved using the finite difference for the hydrostatic balance in the sigma-pressure vertical coordinate. Moreover, the observed weather elements serve as input data for these models creating the initial and boundary conditions needed for the running process.

Since air pollution is one of the most important environmental issues, several studies were devoted for investigating air pollution using RegCM [5, 6, 7]. The

most common pollutants in air are carbon monoxide and dioxide, nitrogen dioxide, sulfur oxide and particulate matter. The sources of air pollutants can be categorized into natural sources and anthropogenic (man-made) sources. Dust storms are a natural source for the particulate matter whose diameters are less than $10\mu\text{m}$, PM10. These suspended particles can get deeply into lungs causing harmful effects to the respiratory system and serious health problems [8, 9].

Transport and dispersion of pollutants occur within the lowest part of the atmosphere, which is known as the planetary boundary layer PBL [10]. Through the turbulent processes within the PBL, fluxes of momentum, heat, moisture and pollutants are transferred from the earth's surface to the higher layers of the atmosphere. Therefore, the different PBL parameterization schemes in the RegCM provide different simulations for the vertical fluxes and diffusion of pollutants in the whole column of the air within the boundary layer [11, 12, 13]. Hence, an efficient parameterization of planetary Boundary layer is essential for more accurate predictions of pollution within the atmosphere.

* Corresponding author e-mail: marwafarouk8313@outlook.com

In this study, the impact of using three different PBL schemes on simulation of a dust storm over Cairo megacity in Egypt is investigated using RegCM4.7. The model performance of the three different PBL schemes will be calibrated through boundary layer height, wind speed, and PM10 concentration. The paper aims to find the best PBL scheme for predicting the PM10 concentration using RegCM4.7 model. Validation of the model results is conducted by comparing the model output and the actual data recorded by Cairo airport station, PM10 stations of Egyptian Meteorological Authority (EMA) and ERA-Interim reanalysis data.

2 Materials and method

2.1 Database

In this study, RegCM4.7 was employed to simulate the dust storm occurred over Egypt in December 2010 with three different PBL schemes and to evaluate the mass concentration levels of PM10 resulted from the storm. The investigated domain extended from latitude 20° E to 39° E and longitude from 15° N to 47° N. The validation of the model output is examined over Cairo, Egypt (31° E, 30° N). Cairo is a megacity and the second largest city in Africa according to its area and population that exceeds 17M inhabitant. For the model output validation, the following insitu measurements were considered:

- Meteorological data from Cairo airport weather reports.
- PM10 measurements from EMA pollution station.
- PBLH from ERA-Interim reanalysis data.

2.2 Model set up and configuration

RegCM4 is a hydrostatic sigma-pressure vertical coordinate regional climate model. It has been used in several studies of climate and dust storms [14]. The reanalysis data ERA-Interim (available source from <https://apps.ecmwf.int/datasets/data/interim-full-daily/levtype=sfc/>) were used as meteorological initial and boundary conditions (ICBC) with resolution of 1.5 degree, its temporal availability was four times daily. Model setup and schemes used in the Model for different simulations of physical processes are shown in Table 1.

Any numerical model used in weather prediction is based on the following dynamical equations:

- Ideal gas law

$$P = \rho RT \quad (1)$$

- Conservation of momentum

$$\frac{\partial V}{\partial t} + V \cdot \nabla V = -\frac{\nabla P}{\rho} - 2\pi \times V + g + F \quad (2)$$

Table 1: Model setup and schemes used in the Model for different simulation of physical processes.

Model	Set up and simulation schemes
Domain	20° E - 39° E longitude and 15° N - 47° N (120 X 120 grid points)
Resolution	20 km
Projection	Lambert Conformal
Vertical levels	18 sigma vertical levels
Atmospheric radiation	NCAR CCM3 Kiehl [15]
Transferred flux from land surface to other higher layers of atmosphere, solar radiation gain, values for wind, moisture, and temperature in the atmosphere	BATS (Biosphere-Atmosphere Transfer Scheme of Dickinson (1993) [16]
Convection over land	Grell scheme (1993) [17]
Convection over ocean	Emanuel scheme (1991) [18]
Sub-grid explicit moisture	Pal. scheme (2000) [19]
Different soil texture distribution from sub-grid emissions	Laurent scheme (2008) [20]
Dust emission size distributions calculations	Alfaro (2001), and Zakey scheme (2004) schemes [21, 22]
PBL schemes	Holtslag, UW, and GFS schemes [23, 24, 25, 26, 27, 28, 29]

- Conservation of mass

$$\frac{\partial \rho}{\partial t} + V \cdot \nabla \rho = -\rho \cdot V \quad (3)$$

- Conservation of energy

$$C_p \left(\frac{\partial T}{\partial t} + V \cdot \nabla T \right) = \frac{1}{\rho} \frac{\partial P}{\partial t} + Q + F_T \quad (4)$$

- Conservation of water content

$$\frac{\partial q}{\partial t} + V \cdot \nabla q = \frac{S_q}{\rho} + F_q \quad (5)$$

where V is the the air velocity, t is the arbitrary time, P is the air pressure, ρ is the air density, g is the gravitational force, F is the friction force, C_p is the specific heat at constant volume, T is the air temperature, Q is the heating rate, F_T is the effect of horizontal diffusion, q is the water vapour mixing ratio, and S_q as well as F_q are tendencies related to the parameterized processes.

Since the primary objective of this study is to evaluate the performance of boundary-layer schemes, a brief description of the three PBL schemes is represented next.

2.2.1 Holtslag scheme

Holtslag scheme is used only inside the PBL. It considers surface heating because incoming solar radiation is the origin of turbulent motion in the PBL [23, 24]. The eddy diffusivity of heat inside the PBL, K_H , is defined by

$$K_H = kW_t z \left(1 - \frac{z}{h}\right)^2 \quad (6)$$

where $k = 0.4$ is the Von Karmon constant, W_t is the turbulent velocity scale, z is the height inside PBL, and h is the PBL height where the condition that the gradient Richardson number R_i equals its critical value of $R_{ic} = 0.25$. Above the PBL, K_H is considered a function of R_i , wind shear and the asymptotic turbulent length scale l_∞ where $l_\infty = 40m$.

$$K_H = K_{H_0} + (R_i(\sigma) - R_{ic}(\sigma)) \cdot l_\infty^2 \cdot \sqrt{\left(\frac{\Delta u}{\Delta z}\right)^2 + \left(\frac{\Delta v}{\Delta z}\right)^2} \quad (7)$$

where σ is the model sigma vertical coordinate, K_{H_0} is the background minimum vertical mixing coefficient. The asymptotic length scale l_∞ in Equation (7) has no unique formulation or value of for vertical mixing above the PBL [25]. The quantity $\Delta z^2 / \Delta t$ is set to be 0.8 above the PBL, where Δz is the layer depth and Δt is the model time step. At the same time, the minimum eddy diffusivity and viscosity are set to a relatively high value of $1m^2s^{-1}$ inside and above the PBL.

2.2.2 University of Washington (UW) Scheme

The UW scheme is a 1.5-order local TKE (Turbulent Kinetic Energy) closure scheme [26]. It considers the region of the increased turbulent activity associated with the buoyancy perturbations because of the cloud-top entrainment instability and longwave cooling present at the stratocumulus (low level type of clouds) -topped PBLs [10].

The eddy heat diffusivity K_H is related to the TKE [27]:

$$K_H = l \sqrt{2TKE} \cdot S_H \quad (8)$$

where S_H is the stability function and l is the master turbulent length scale with two options found in RegCM. In convective boundary layers, one of the two following formulations for l can be chosen in initial model setup:

$$l_1 = \frac{\min(kz, 0.1\Delta z)}{1 + \frac{\min(kz, 0.1\Delta z)}{\lambda}} \quad (9)$$

$$l_2 = \min(kz, 0.1\Delta z) \quad (10)$$

where λ is the asymptotic master turbulent length scale, $\lambda = 0.085\Delta z$, Δz is the depth of the convective sub-layer. For the same z and Δz , l_2 is larger than l_1 and the use of l_2 increases eddy heat diffusivity K_H Equation (8). In stably stratified conditions,

$$l_1 = l_2 = \min(R_{STBL} \sqrt{\frac{TKE}{N^2}}, kz) \quad (11)$$

It means that no difference exists in the formulation of the master length, N is buoyancy frequency and R_{STBL} is a scaling factor. Only at the top of the cloud-topped PBL the following closure for the eddy heat diffusivity is assumed

$$K_H = w_e \Delta_i z \quad (12)$$

where w_e is the entrainment rate, and $\Delta_i z$ is the change in depth of the entrainment layer.

As a part of the UW scheme, an additional prognostic equation for TKE is implemented where the local change of TKE is governed by buoyancy production and destruction, shear production, turbulent vertical transport and turbulent dissipation [26]. TKE horizontal, vertical advection and horizontal diffusion are given by the following equation:

$$\begin{aligned} \frac{\partial TKE}{\partial t} + \vec{u} \cdot \vec{\nabla} TKE + w \frac{\partial TKE}{\partial z} = \\ -K_H N^2 + K_M S_f^2 + \frac{\partial}{\partial z} \left(K_{TKE} \frac{\partial TKE}{\partial z} \right) - \\ B_1 \frac{TKE^{3/2}}{l} + D \end{aligned} \quad (13)$$

where K_M and K_{TKE} are the momentum and TKE turbulent diffusivities respectively, S_f^2 is the wind shear squared, B_1 is a constant in the turbulent dissipation term and D is horizontal diffusion term.

In the RegCM implementation of Equation (13), vertical gradient and vertical velocity are transformed to the sigma vertical coordinate system. The inclusion of the TKE prognostic equation increases the RegCM computational requirements only moderately (e.g. simulations with the UW scheme take approximately 30% more computer time compared to those with the Holtslag scheme) [30].

2.2.3 The Global Forecast System (GFS) scheme

The GFS is a weather forecast model produced by the National Centers for Environmental Prediction (NCEP) [28]. GFS is a coupled model, composed of an atmosphere model, an ocean model, a land/soil model, and a sea ice model which work together to provide an accurate picture of weather conditions. The scheme is a first-order non local vertical diffusion scheme. One of its features is to diagnostically determine PBL height (PBLH) using the bulk-Richardson approach to iteratively estimate PBLH starting from the ground upward. Once

the PBLH is defined, the profile of the coefficient of diffusivity is specified as a cubic function of the PBLH. The actual values of the coefficients are determined by matching with the surface-layer fluxes. There is also a counter-gradient flux parameterization (for temperature only) representing the non local mixing done by the largest PBL eddies that is based on the fluxes at the surface and the convective velocity scale [29]. As the PBL stability conditions differ during daytime from night, the vertical heat flux is given by:

- during the daytime:

$$\overline{w'\theta'} = -(K_h^{surf} + K_h^{sc}) \frac{\partial \bar{\theta}}{\partial z} + K_h^{surf} \gamma_h \quad (14)$$

- during the night:

$$\overline{w'\theta'} = -(K_h(R_i) + K_h^{sc}) \frac{\partial \bar{\theta}}{\partial z} \quad (15)$$

where K_h^{surf} and K_h^{sc} are the surface and cloud-top eddy diffusivities, $\bar{\theta}$ is the average Kinematic heat flux, γ_h is the nonlocal countergradient mixing term due to non-local convective eddies, and $K_h(R_i)$ is the mixing coefficient based on the local Richardson number. The presence of the term K_h^{sc} in Equation (15) displays a larger vertical heat flux in the stratocumulus regions. The vertical diffusivity for momentum, surface driven diffusion, is given by

$$K_m^{surf} = K w_s z \left(1 - \frac{z}{h}\right)^2 \quad (16)$$

where w_s is the velocity scale. The diffusivity coefficients for momentum and heat are written in terms of the mixing length l , stability functions $f_{m,h}(R_i)$, and the vertical wind shear component magnitude $|\frac{\partial U}{\partial z}|$, as

$$K_{m,h}(R_i) = l^2 f_{m,h}(R_i) \left| \frac{\partial U}{\partial z} \right| \quad (17)$$

The mixing length l is expressed by

$$\frac{1}{l} = \frac{1}{kz} + \frac{1}{l_0} \quad (18)$$

where l_0 is the length scale and

$$l_0 = \begin{cases} 30m & \text{for stable conditions} \\ 150m & \text{for unstable conditions} \end{cases} \quad (19)$$

The stability functions $f_{m,h}(R_i)$ are functions of the local gradient Richardson number.

3 Results

Since the dust events are considered as a major natural source for PM10, the case study under consideration was

chosen to be the sand storm that hit Egypt on 11th, 12th and 13th of December 2010. The first and second days represented the peak of the storm. However, one day before and after the dust storm was considered in the study. Verification and validation of the model output were examined by calculating the mean bias error (MBE), root mean squared error (RMSE), and mean absolute percentage error (MAPE).

3.1 Wind speed

Wind speed is one of the factors that cause motion within the PBL to be a turbulent motion, so it affects the PBL thickness. High wind speed is responsible for transporting pollutants from one place to another, and reducing the concentration of the pollutant in the atmosphere.

During the peak of the storm, wind speed exceeded 12m/s. Compared with the actual wind speed recorded by EMA, the output of the model's PBL schemes of wind speed shown in Figure 1 came to be accurate with a prediction percentage error shown in Table 2.

The results of Holtslag PBL scheme came to be more accurate than those of the other two schemes.

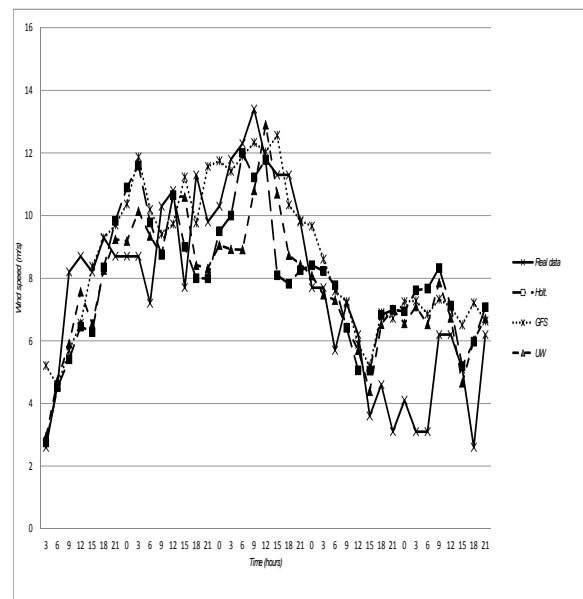


Fig. 1: The actual wind speed (m/s) vs. three schemes output wind speed.

3.2 PM10 concentration

Figure 2 illustrates the levels of PM10 on the five days considered by the study. It is noticeable that PM10 levels

Table 2: Statistical measures: MBE, RMSE and MAPE measures for the validation of the wind speed output compared to the real data.

Wind speed (m/s)	Holslag	UW	GFS
MBE	-0.64	-1.02	0.85
RMSE	1.7	2.4	1.9
MAPE (%)	6.5%	11.2%	7.4%

are much higher at the days of the storm than the other days. The allowed average daily concentration dosage is $50\mu\text{g}/\text{m}^3$ per day according to the WHO air quality guidelines [9].

On the first day before the storm PM10 concentration was around its normal levels as for crowded polluted megacity like Cairo, it was tolerable to exceed the allowed mean daily concentration by some certain percentage by about 20-40% of the mean daily dosage. During the peak period, the PM10 concentration levels raised above the permitted levels as shown in Figure 2. That was very harmful to the people suffering from respiratory diseases. Upon this prediction EMA made a report to warn the citizens of the bad weather that impedes driving on desert roads and outdoor activities. The comparison between the three PBL schemes results revealed that Holslag scheme was much better than the other two schemes compared to the real data as shown in Table 3.

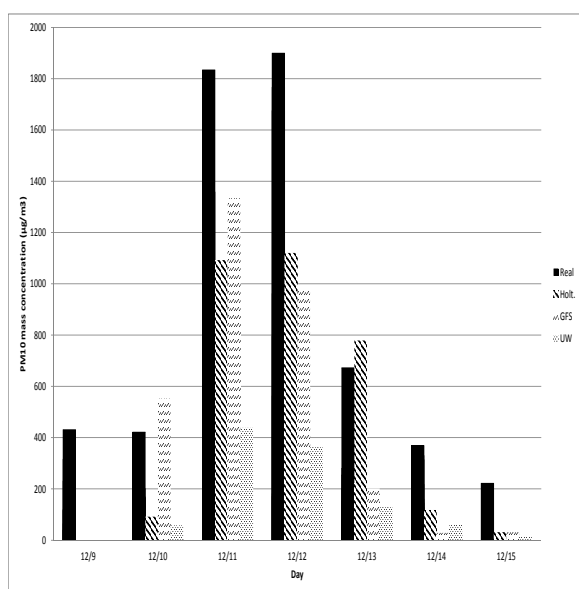


Fig. 2: Comparison between the PM10 concentration output of the three PBL schemes and the real data.

Table 3: Statistics of PM10 concentration between RegCM4.7 PBL schemes and observations (real data) with the Performance indicators root mean squared error (RMSE), and mean absolute percentage error (MAPE).

PM10 ($\mu\text{g}/\text{m}^3$)	Holslag	UW	GFS
RMSE	14.05	75.26	55.23
MAPE (%)	26.3%	68.4%	40.2%

3.3 Boundary layer height (PBLH)

The turbulent process within the PBL is responsible for the transport of fluxes from the earth’s surface to the higher layers above vertical mixing. The relation between the PBLH and vertical mixing affects the dilution of pollutants emitted near the ground and the near-surface air quality [31, 32, 33]. The more the turbulence, the higher the PBL and the less the pollutants concentration. The real data used in this section to calibrate the PBLH output is the reanalysis data taken from ERA- Intrem data. According to the model output, the PBLH recorded a significant increase in its height during the sand storm as shown in Figure 3. Accuracy of the Holslag scheme results was higher than that of the other two schemes as shown in Table 4.

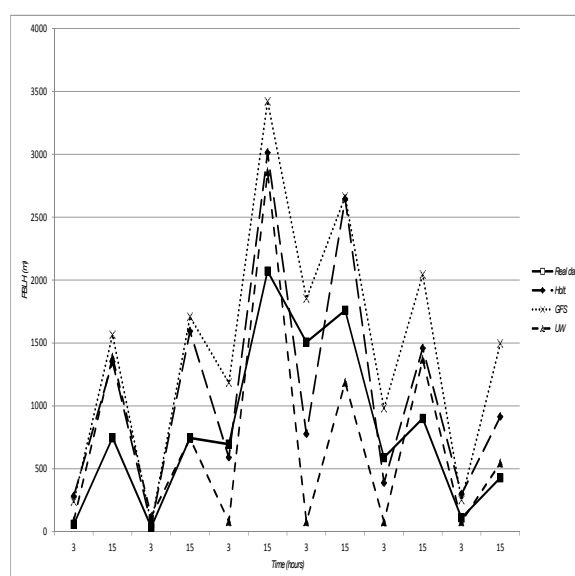


Fig. 3: Comparison between PBLH for the three schemes output and the reanalysis data.

Table 4: Statistical measures: MBE, RMSE and MAPE measures for the validation of the PBLH model out put compared to the ERA-intrem data.

PBLH (m)	Holslag	UW	GFS
MBE	286.50	-311.62	300.12
RMSE	16.92	21.48	18.32
MAPE (%)	18.92%	24.85%	21.35%

3.4 The consistency of the model

Consistency of the model performance was examined through highlighting the relation among PBLH, wind speed, and the dispersion of PM10 as a pollutant. As the wind becomes stronger, the PBLH increases and more turbulence occurs. Thus, the concentration of pollutants minimizes. Figures 4 and 5 show that there is a negative correlation between PM10 concentration and wind speed, which is consistent with the general concept of the turbulent motion and air pollution.

3.5 Ventilation index

Ventilation index is a common term used in air pollution. It represents the relation among wind speed, PBLH and air pollution quality control. It is a numerical value related to the dispersing potential for airborne pollutants in a certain local of the atmosphere. Ventilation index (VI) was calculated according to the following formula

$$VI = \frac{\sqrt{windspeed \times mixinglayerheight}}{10} \quad (20)$$

It is based on both the height (thickness) of the mixed PBL layer and the existing wind in this layer. Stronger wind speed and thicker mixed layer will produce good dispersion which reduces the concentration of pollutants and provides healthier conditions that means higher ventilation index. Table 5 shows that the maximum ventilation index is recorded during the maximum wind speed and the maximum PBLH.

Table 5: Relation between ventilation index (VI), wind speed (WS) and PBLH.

Schemes	Max. VI	Max. WS (m/s)	Max. PBLH (m)
Holslag	10.65	10.65	3013.20
UW	10.79	10.86	2860.45
GFS	14.02	12.03	3421.13

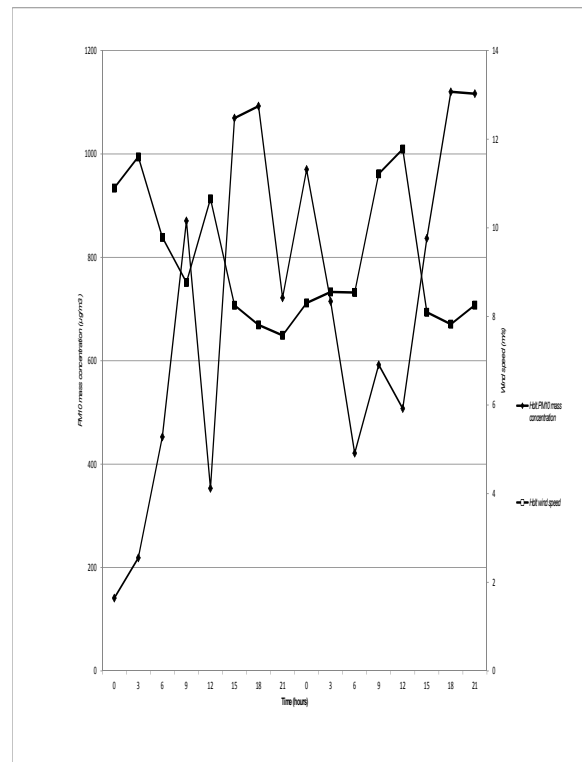


Fig. 4: Scattered plot of PM10 mass concentration ($\mu\text{g}/\text{m}^3$) and wind speed (m/s).

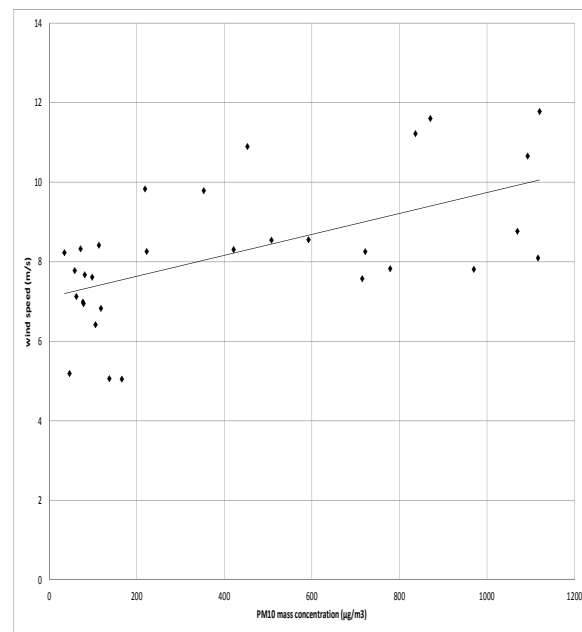


Fig. 5: Diurnal variation of PM10 mass concentration ($\mu\text{g}/\text{m}^3$) and wind speed (m/s).

4 Conclusion

In this paper, an experiment was accomplished to investigate using the numerical model RegCM4.7 to predict the PM10 mass concentration levels originated by a sand storm over Egypt. As the pollutant dispersion occurred within the planetary boundary layer PBL, it was focused on three PBL schemes for running the model (Holtslag, UW and GFS). The results showed that the model gave a good representation for the case study. Concerning the PM10 concentration, the results of Holtslag scheme were more accurate than those of UW and GFS schemes. Consistency of the model was also examined and the results of the relation between the wind speed, PBLH and PM10 concentration were proved during the sand storm. Hence we conclude that strong wind speed and thick PBL layer produced a good dispersion of pollutants which consequently reduced the concentration of the PM10, gave healthier conditions and produced higher ventilation index.

Acknowledgment

The authors thank Egyptian Meteorological Authority where the PM10 data were obtained.

The authors are grateful to the anonymous referee for the careful checking of the details and the constructive comments that improved this paper.

Conflicts of Interest

The authors declare that there is no conflict of interest regarding the publication of this article.

References

- [1] Eugenia Kalnay. *Atmospheric modeling, data assimilation and predictability*. Cambridge university press, 2003.
- [2] Robert E Dickinson, Ronald M Errico, Filippo Giorgi, and Gary T Bates. A regional climate model for the western united states. *Climatic change*, 15(3):383–422, 1989.
- [3] Filippo Giorgi and Gary T Bates. The climatological skill of a regional model over complex terrain. *Monthly Weather Review*, 117(11):2325–2347, 1989.
- [4] Filippo Giorgi, E Coppola, F Solmon, L Mariotti, MB Sylla, X Bi, N Elguindi, GT Diro, V Nair, G Giuliani, et al. Regcm4: model description and preliminary tests over multiple cordex domains. *Climate Research*, 52:7–29, 2012.
- [5] Tugba Agacayak, Tayfun Kindap, Alper Unal, Luca Pozzoli, Marc Mallet, and Fabien Solmon. A case study for saharan dust transport over turkey via regcm4. 1 model. *Atmospheric Research*, 153:392–403, 2015.
- [6] Amira N Mostafa, Ashraf S Zakey, Stephane C Alfaro, Ali A Wheida, Soltan A Monem, and Mohamed M Abdul Wahab. Validation of regcm-chem4 model by comparison with surface measurements in the greater cairo (egypt) megacity. *Environmental Science and Pollution Research*, 26(23):23524–23541, 2019.
- [7] Marwa Farouk M Ali, Somia A Askalany, M Abd El-wahab, and MA Hassan. Data mining algorithms for weather forecast phenomena: Comparative study. *IJCSNS*, 19(9):76, 2019.
- [8] Ziqiang Meng and Bin Lu. Dust events as a risk factor for daily hospitalization for respiratory and cardiovascular diseases in minqin, china. *Atmospheric environment*, 41(33):7048–7058, 2007.
- [9] World Health Organization. *Air quality guidelines: global update 2005: particulate matter, ozone, nitrogen dioxide, and sulfur dioxide*. World Health Organization, 2006.
- [10] Roland B Stull. *An introduction to boundary layer meteorology*, volume 13. Springer Science & Business Media, 2012.
- [11] William C Skamarock, Joseph B Klemp, Jimmy Dudhia, David O Gill, Dale M Barker, Michael G Duda, Xiang-Yu Huang, Wei Wang, and Jordan G Powers. G.: A description of the advanced research wrf version 3. In *NCAR Tech. Note NCAR/TN-475+STR*. Citeseer, 2008.
- [12] P Ajay, Binita Pathak, F Solmon, PK Bhuyan, and F Giorgi. Obtaining best parameterization scheme of regcm 4.4 for aerosols and chemistry simulations over the cordex south asia. *Climate dynamics*, 53(1-2):329–352, 2019.
- [13] Bhishma Tyagi, Vincenzo Magliulo, Sandro Finardi, Daniele Gasbarra, Pantaleone Carlucci, Piero Toscano, Alessandro Zaldei, Angelo Riccio, Giuseppe Calori, Alessio D’Allura, et al. Performance analysis of planetary boundary layer parameterization schemes in wrf modeling set up over southern italy. *Atmosphere*, 9(7):272, 2018.
- [14] Sara Basart, Carlos Pérez, Slodoban Nickovic, Emilio Cuevas, and JoséMARÍA Baldasano. Development and evaluation of the bsc-dream8b dust regional model over northern africa, the mediterranean and the middle east. *Tellus B: Chemical and Physical Meteorology*, 64(1):18539, 2012.
- [15] JT Kiehl, JJ Hack, GB Bonan, BA Boville, DL Williamson, and PJ Rasch. The national center for atmospheric research community climate model: Ccm3. *Journal of Climate*, 11(6):1131–1149, 1998.
- [16] E Dickinson, A Henderson-Sellers, and J Kennedy. Biosphere-atmosphere transfer scheme (bats) version 1e as coupled to the near community climate model. 1993.
- [17] Georg A Grell. Prognostic evaluation of assumptions used by cumulus parameterizations. *Monthly weather review*, 121(3):764–787, 1993.

- [18] Kerry A Emanuel. A scheme for representing cumulus convection in large-scale models. *Journal of the Atmospheric Sciences*, 48(21):2313–2329, 1991.
- [19] Jeremy S Pal, Eric E Small, and Elfatih AB Eltahir. Simulation of regional-scale water and energy budgets: Representation of subgrid cloud and precipitation processes within regcm. *Journal of Geophysical Research: Atmospheres*, 105(D24): 29579–29594, 2000.
- [20] B Laurent, B Marticorena, G Bergametti, JF Léon, and NM Mahowald. Modeling mineral dust emissions from the sahara desert using new surface properties and soil database. *Journal of Geophysical Research: Atmospheres*, 113(D14), 2008.
- [21] Stéphane C Alfaro and Laurent Gomes. Modeling mineral aerosol production by wind erosion: Emission intensities and aerosol size distributions in source areas. *Journal of Geophysical Research: Atmospheres*, 106(D16):18075–18084, 2001.
- [22] AS Zakey, F Solmon, and F Giorgi. Development and testing of a desert dust module in a regional climate model. 2006.
- [23] AAM Holtslag, EIF De Bruijn, and HL Pan. A high resolution air mass transformation model for short-range weather forecasting. *Monthly Weather Review*, 118(8):1561–1575, 1990.
- [24] AAM Holtslag and BA Boville. Local versus nonlocal boundary-layer diffusion in a global climate model. *Journal of Climate*, 6(10):1825–1842, 1993.
- [25] Roger A Pielke Sr, Toshihisa Matsui, Giovanni Leoncini, Timothy Nobis, Udaysankar S Nair, Er Lu, Joseph Eastman, Sujay Kumar, Christa D Peters-Lidard, Yudong Tian, et al. A new paradigm for parameterizations in numerical weather prediction and other atmospheric models. *National Weather Digest*, 30:93–99, 2006.
- [26] Hervé Grenier and Christopher S Bretherton. A moist pbl parameterization for large-scale models and its application to subtropical cloud-topped marine boundary layers. *Monthly weather review*, 129(3): 357–377, 2001.
- [27] P Monti, HJS Fernando, M Princevac, WC Chan, TA Kowalewski, and ER Pardyjak. Observations of flow and turbulence in the nocturnal boundary layer over a slope. *Journal of the Atmospheric Sciences*, 59 (17):2513–2534, 2002.
- [28] IB Troen and L Mahrt. A simple model of the atmospheric boundary layer; sensitivity to surface evaporation. *Boundary Layer Meteorology*, 37(1-2): 129–148, 1986.
- [29] Song-You Hong and Hua-Lu Pan. Nonlocal boundary layer vertical diffusion in a medium-range forecast model. *Monthly weather review*, 124(10):2322–2339, 1996.
- [30] Ivan Güttler, Čedo Branković, Travis A O'Brien, Erika Coppola, Branko Grisogono, and Filippo Giorgi. Sensitivity of the regional climate model regcm4. 2 to planetary boundary layer parameterisation. *Climate dynamics*, 43(7-8):1753–1772, 2014.
- [31] DHP Vogelezang and AAM Holtslag. Evaluation and model impacts of alternative boundary-layer height formulations. *Boundary-Layer Meteorology*, 81(3-4): 245–269, 1996.
- [32] Gaurav Govardhan, Ravi S Nanjundiah, SK Satheesh, K Krishnamoorthy, and VR Kotamarthi. Performance of wrf-chem over indian region: Comparison with measurements. *Journal of Earth System Science*, 124 (4):875–896, 2015.
- [33] AK Blackadar. Modeling pollutant transfer during daytime convection. In *Preprints Fourth Symposium on Atmospheric Turbulence, Diffusion and Air Quality. Reno. Amer. Met. Soc., 1978*, pages 443–447. Amer. Met. Soc., 1978.



M. Farouk received the MSc degree in Mathematics at Ain Shams University, Egypt. Her research interests are in the areas of mathematics, modelling including mathematical physics, atmospheric science and numerical models for weather and climate research.

She is One of the Egyptian Meteorological authority members participated in published research articles in reputed international journals of Computer science and network security.



Zeinab Salah is a Researcher in Egyptian Meteorological Authority, in numerical weather prediction center (2008-2012), in the air pollution (2012-present), Postdoctoral research fellow (2015-2016) in Environmental Physical Laboratory (EPhysLab),

Facultad de Ciencias de Ourense, Universidad de Vigo. B.Sc. in Physics- Ain Shams University 2003. Diploma of Meteorology- Cairo University 2005. M.Sc. in Meteorology in the conditions of atmospheric stability over Egypt- Cairo University 2008. PhD in Meteorology for Aerosol indirect effects in the regional climate model - Cairo University, 2014. Her research interest is climate modeling, air quality and climate change.



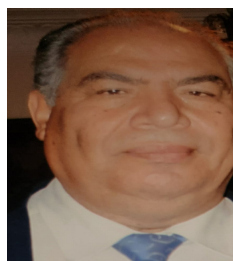
Somaia A. Asklany is an assistant professor, Computer science department, Northern Border University King Saudi Arabia. Bs.c in Computer science and mathematics Minia University 1992, MSc in numerical modeling 2006 for building application numerical prediction help in

in studying the behavior of pollutant diffusion and Ph.D in Expert systems Cairo University 2011 to create expert systems based on intelligent approaches: fuzzy logic and neural networks. Her research interest is artificial intelligence application in area of modeling, data science and prediction techniques.



M. Harhash received her MSc and PhD degrees in Meteorology at Cairo University, Egypt. Her research interests are in the areas of atmospheric science including mathematical physics, remote sensing, and numerical models for weather and climate research. She has

participated in published research articles in reputed international journals of energy, atmospheric sciences, and applied mathematics.



Mohamed Hassan is a professor of mathematics for more than 30 years, faculty of science, Ain Shams University . His research interests are: three-body force effect, unstable nuclei, half-life time, Suggested formulas, high energies, hadron-deuteron elastic scattering, optical limit

approximation, and field of numerical modelling.



M. M. Abdel Wahab has over 35 years of experience in the field of meteorology and atmospheric science. He is specialized in weather modelling, climate change and air pollution. He is currently teaching and consulting in these fields. He has been a Principle Investigator and co-Director

of many scientific projects including the establishing of an Earth Observation satellite data receiving station at Cairo University (funded by NATO Science for Peace program). He was leading some international projects with co-partners from Italy, France, Switzerland, USA (NCAR) and Purdue University. Recently Dr. Wahab has been engaged with ionospheric physics simulations and space weather problems. He is a member in Third National Communication Report Team. He is the responsible for the Adaptation Strategy INDCs.